Imaging of T-cell receptor fused to CD3ζ reveals enhanced expression and improved pairing in living cells

CHANGLI TAO[1,2*], HONGWEI SHAO[2*], YIN YUAN[2], HUI WANG[2], WENFENG ZHANG[2], WENLING ZHENG[1], WENLI MA[1] and SHULIN HUANG[2]

[1]Institute of Genetic Engineering, Southern Medical University, Guangzhou, Guangdong 510515; [2]Guangdong Province Key Laboratory for Biotechnology Drug Candidates, School of Life Science and Biopharmaceutics, Guangdong Pharmaceutical University, Guangzhou, Guangdong 510006, P.R. China

Received March 10, 2014; Accepted June 27, 2014

DOI: 10.3892/ijmm.2014.1839

Abstract. T cell receptor (TCR) gene adoptive therapy is a promising clinical approach for the treatment of malignant tumors and viral diseases. However, the effectiveness of this strategy is hampered by the generation of mixed TCR heterodimers comprising both exogenous and endogenous TCR chains (i.e., mispairing of TCR chains). In the present study, we constructed genetically encoded reporters fused to a pair of fluorescent proteins [enhanced cyan fluorescent protein (ECFP)/enhanced yellow fluorescent protein (EYFP)] to monitor the expression of TCRαζβζ and pairing between TCRαζ and TCRβζ. We demonstrate that these reporters provide accurate images of TCRαζβζ expression, which is markedly stronger with evident microclusters accumulated at the plasma membrane compared to wild-type (wt)TCR. Using fluorescence resonance energy transfer (FRET) analysis, we demonstrate that, in addition to the improved pairing, the expression and assembly of TCRαζβζ are independent of endogenous CD3 subunits. These results suggest that the fusion genes, TCRαζ and TCRβζ, coupled to ECFP and EYFP, respectively can effectively monitor the expression and interaction in cells. Our data suggest a novel strategy with which it is possible to effectively express and pair TCRαζβζ, thus making TCR gene adoptive therapy more effective.

Correspondence to: Professor Shulin Huang, Guangdong Province Key Laboratory for Biotechnology Drug Candidates, School of Life Science and Biopharmaceutics, Guangdong Pharmaceutical University, 280 E. Road, Guangzhou Higher Education Mega Center, Guangzhou, Guangdong 510006, P.R. China
E-mail: shulhuang@sina.com

Professor Wenli Ma, Institute of Genetic Engineering, Southern Medical University, 1838 Guangzhou Avenue North, Guangzhou, Guangdong 510515, P.R. China
E-mail: wenli668@gmail.com

*Contributed equally

Key words: T cell receptor, mispairing, fluorescence resonance energy transfer, TCRαζβζ, CD3ζ, T-cell receptor gene therapy

Introduction

Antigen-specific TCR gene transfer enables the instantaneous generation of defined T cell immunity and TCR gene-modified T cells are fully functional *in vitro* and in murine models (1-6). The retroviral transfer of a MART1-specific TCR for adoptive T cell therapy first used in clinical trials on melanoma patients demonstrated the feasibility of TCR gene therapy (7,8). However, several factors currently limit the efficacy and hamper the application of TCR gene immunotherapy. One of these critical issues is that the introduced TCRα and β chain can potentially assemble with endogenous TCR chains (i.e., TCR mispairing), which not only reduces the expression of the desired TCR pair, but can create a new TCR with unknown specificity that can potentially cause autoimmunity and off-target toxicity (9,10).

A number of strategies have been investigated to prevent the mixed TCR dimer formation. Examples of such strategies are the replacement of the C domains of the TCRα and β chains by the corresponding murine domains (11,12), introduction of an additional inter-chain disulfide bond between the constant domains of TCRα and β chains (13,14), the inversion of amino acid residues in the constant region of the TCRα and β chains that form the TCR interface (15), and the use of single-chain TCR (scTCR) chimeras, including three-domain TCRs that contain other signaling domains, such as CD3ζ or FcεRIγ (VαVβCβCD3ζ) (16-18). However, the full extent to which these strategies can prevent TCR chain mispairing is unclear.

In a recent study, we have isolated a TCR (Vα12 and Vβ7) from tumor infiltrating lymphocytes (TILs) of patients (HLA-A^{2+} and AFP^{+}) with hepatocellular carcinoma (19). We demonstrated that T cells derived from central memory cells modified by tumor-specific TCR gene transfer were more effective than T cells derived from $CD8^{+}$ T cells modified by TCR gene transfer in inducing CTL activity and effector cytokine secretion. However, wild-type (wt)TCRα12 and β7 expression in transduced human T cells was lower than the levels of endogenous TCR chains, mispairing with the endogenous TCR.

In the present study, we generated a chimeric TCRαζβζ which was modified by fusing the original constant domains downstream of the extracellular cysteine of wtTCRα and β chains to complete human CD3ζ. Subsequently, we constructed genetically encoded reporters coupled with a pair of fluorescent proteins to monitor the expression of TCRαζβζ and pairing between TCRαζ and TCRβζ using confocal laser scanning microscopy (CLSM) in living cells (Jurkat and BEL-7402 cells). We demonstrate that these reporters provide accurate images of TCRαζβζ expression and pairing. Of note, we observed that the expression of TCRαζβζ was markedly stronger and with evident microclusters accumulated at the plasma membrane compared to wtTCRαβ. Fluorescence resonance energy transfer (FRET) imaging analysis of the T cells and non-T cells revealed that the expression of TCRαζβζ does not need the engagement of CD3 subunits. Using these reporters, we demonstrate that in addition to enhanced pairing, TCRαζβζ expression is greater in T cells or non-T cells without CD3 subunits. Taken together, these results suggest the reporters we used are usseful in studying the expression/pairing of TCRαζβζ, which may be an effective approach to preventing mispairing in TCR gene therapy.

Materials and methods

Cells, genes and reagents. Jurkat/E6-1 (ATCC TIB-152) cells were cultured in RPMI-1640 medium (Gibco/Invitrogen, Carlsbad, CA, USA), human embryonic kidney cells (HEK293) and human hepatocellular carcinoma cells (BEL-7402; maintained in our laboratory) were cultured in Dulbecco's modified Eagle's medium (DMEM) (Gibco/Invitrogen). All cultures were supplemented with 10% fetal bovine serum (FBS; Gibco/Invitrogen), 100 U/ml streptomycin and 100 U/ml penicillin. The TCRα12 and β7 chains were isolated from TILs of patients (HLA-A^{2+} and AFP^{+}) with hepatocellular carcinoma by our laboratory as previously described (19). CD3ζ chains were isolated from peripheral blood mononuclear cells (PBMCs) of a healthy donor (GenBank accession no. NM_000734.3). The pair of fluorescent proteins [enhanced cyan fluorescent protein (ECFP)/enhanced yellow fluorescent protein (EYFP)] was kindly provided by Dr G. Zhang (Guangzhou University of Chinese Medicine, Guangzhou, China). Monoclonal antibodies (mAbs) used for flow cytometry included FITC-conjugated anti-TCRVα12.1 mAb (Pierce Biotechnology, Rockford, IL, USA) and PE-conjugated anti-TCRVβ7.1 (Beckman Coulter, Brea, CA, USA).

Splice overlap extension (SOE) PCR. The strategy for the tripartite DNA fragment fusion by SOE PCR is shown in Fig. 2A. Variable fragments for generating TCRαζ-ECFP (including TCRα, CD3ζ-a and EYFP) and TCRβζ-EYFP (including TCRβ, CD3ζ-b and ECFP) were amplified using a set of forward primers and reverse primers. The first step of SOE PCR reactions was performed with 100 ng (3 fragments were mixed with an equimolar ratio) of template without primers, 10X Buffer, 2 mM dNTPs, 25 mM $MgSO_4$, 0.5 U KOD-Plus-Neo Polymerase in a 25 μl reaction volume. The PCR cycling conditions were as follows: initial denaturation at 94˚C for 2 min, followed by 5 cycles at 94˚C for 30 sec, at 57˚C for 30 sec and at 68˚C for 1.5 min and completed with a final extension at 68˚C for 7 min. This initial PCRs generate overlapping gene segments that are then used as template DNA for the second step of SOE PCR to create a full-length product. Therefore, another 25 μl reaction mixture (containing 10X Buffer, 2 mM dNTPs, 25 mM $MgSO_4$, 0.5 KOD-Plus-Neo Polymerase and 1 μM forward primer P1/P1' and reverse primer P6/P6') was added to the first reaction mixture for the second step of SOE PCR. The reaction conditions were initial denaturation at 94˚C for 2 min, followed by 30 cycles at 94˚C for 30 sec, at 62˚C for 30 sec, and at 68˚C for 1.5 min and a final extension at 68˚C for 7 min, 2 μl of the amplicons were analyzed by agarose gel electrophoresis (1.0%) (Fig. 2B and C). Primer sequences for the amplification of variable regions and fusion chains are presented in Table I. The wtTCRα-ECFP and wtTCRβ-EYFP fusing sequences were generated using the same methods.

Vector construction. To construct a bicistronic vector expressing both the TCRαζ-ECFP and TCRβζ-EYFP chains, the fusion sequences TCRαζ-ECFP and TCRβζ-EYFP were cloned into the original pIRES2-EGFP vector (Clontech Laboratories, Inc., Palo Alto, CA, USA). The TCRαζ-ECFP fusion gene was inserted into the *Bst*XI/*Not*I restriction site of the pIRES2-EGFP vector (Clontech Laboratories), located downstream of an internal ribosomal entry site (IRES) sequence of the plasmid to replace the EGFP gene, then the TRBζ-EYFP fusion gene was inserted into the *Nhe*I/*Sal*I restriction site, located upstream of IRES. The other bicistronic vector expressing both non-modified wtTCRα-ECFP and wtTCRβ-EYFP was constructed in a manner similar to the above-mentioned procedure. The single vectors expressing TCRα-ECFP or TCRβ-EYFP which were used to remove the spectral bleed-through (SBT) contamination in the FRET images were constructed as previously described (20). The identity of all constructs was verified by direct sequencing.

Production of adenoviral particles and the transduction of TCR gene into Jurkat cells. We used the Ad5F35 chimeric adenoviral vector (21) which contained the Ad35 fiber knob incorporated into an Ad5 capsid as the packaging vector, and the whole wtTCRαβ cassette (TCRβ-IRES-TCRα) and TCRαζβζ cassette (TCRβζ-IRES-TCRαζ) was cloned into the shuttle plasmid (pDC315) (Fig. 4A). Adenoviral particles were produced by co-transfection of the packaging cells, HEK293, with Ad5F35 vector and recombinant pDC315, containing wtTCRαβ or TCRαζβζ. The virus-containing supernatants were filtered through 0.45-μm filters. Adenoviral particle titers were determind by the 50% tissue culture infectious dose (TCID50) method and the supernatants were directly used for the infection of the target Jurkat T cells. For Jurkat T cell transduction, 6-well plates were seeded with Jurkat cells at $1x10^6$ cells/well in 2 ml of RPMI 1640 medium supplemented with 2% FBS, cultured for 35 min, and then transduced with MOI 100 PFU of wtTCRαβ or TCRαζβζ viral supernatants. Following culture for 24 h at 37˚C with 5% CO_2, the culture medium was replaced with RPMI 1640 medium supplemented with 10% FBS. After a further 48-h culture period, the cells were analyzed for TCR expression by flow cytometry.

Flow cytometry. The TCR-transduced Jurkat T cells ($5x10^5$) were analyzed for transgene expression by flow cytometry using

Table I. Primers for amplifying 6 gene fragments (regular PCR and SOE PCR).

Fragments	Primers	Sequences (5'→3')
TCRα	P1	ACGCCACAACCTTGGCCACCATGATATCCTTGAGAGTT
	P2	CAGCAGGCCAAAGCTCTGTGGGCTGGGGAAGAAGGTGT
CD3ζ-a	P3	ACACCTTCTTCCCCAGCCCACAGAGCTTTGGCCTGCTG
	P4	TCGCCCTTGCTCACCATGCGAGGGGGCAGGGCCTG
ECFP	P5	CAGGCCCTGCCCCCTCGCATGGTGAGCAAGGGCG
	P6	AGTGCGGCCGCTTACTTGTACAGCTCGTCCAT
TCRβ	P1'	ATAGCTAGCGCCACCATGGGCTGCAGGCTGCTCTG
	P2'	ATCCAGCAGGCCAAAGCTCTGTGCTCTACCCCAGGC
CD3ζ-b	P3'	GCCTGGGGTAGAGCACAGAGCTTTGGCCTGCTGGAT
	P4'	TCGCCCTTGCTCACCATGCGAGGGGGCAGGGCCTG
EYFP	P5'	CAGGCCCTGCCCCCTCGCATGGTGAGCAAGGGCG
	P6'	CGGCGTCGACTTACTTGTACAGCTCGTC

Restriction enzyme sites are underlined.

FITC-conjugated anti-TCRVα12 mAb and PE-conjugated anti-TCRVβ7 mAbs. The cells were incubated with the mAbs on ice for 30 min. Subsequently, the Jurkat cells were washed twice with PBS and centrifuged for 10 min at 1000 x g, and the cell pellet was resuspended and fixed with 2% paraformaldehyde before taking measurements on an Epics XL flow cytometer (Beckman Coulter). The samples were analyzed using EXPO32 software (Beckman Coulter) and are displayed as dotplots.

Imaging by CLSM. The recombinant vectors, pIRES-TCRβ-EYFP/TCRα-ECFP and pIRES-TCRβζ-EYFP/TCRαζ-ECFP, were transfected into the Jurkat and BEL-7402 cells using Lipofectamine LTX/PLUS (Invitrogen) according to the manufacturer's instructions. The cells transfected with pIRES-TCRα-ECFP and pIRES-TCRβ-EYFP were used as controls to remove the SBT contamination in FRET analysis. After 24 h of transfection, the Jurkat cells grown on glass-bottom dishes were washed twice with PBS and immobilized with 0.05% low metling agarose for 15 min and the BEL-7402 cells were washed twice with PBS solution. Confocal images of the cells were acquired using an Olympus FluoView 1000 confocal laser scanning microscope with FV10-ASW 1.7 software (Olympus, Tokyo, Japan). The FRET donor (TCRα-ECFP or TCRαζ-ECFP) was excited with a 458 nm Ar-laser and the acceptor (TCRβ-EYFP or TCRβζ-EYFP) was excited with a 515 nm Ar-laser. The cells were scanned from 475 to 585 nm with a 10 nm step-size and 20 nm band-width to obtain original images.

FRET analysis. FRET efficiency was analyzed using the sensitized acceptor emission (SE) method. FRET occurs when 2 fluorophores (donor and acceptor) have sufficiently large spectral overlap which results in the energy of the donor fluorescence transferring to the acceptor. The spectral overlap between donor and acceptor fluorophores also causes FRET signal contamination, termed SBT. It is important to remove

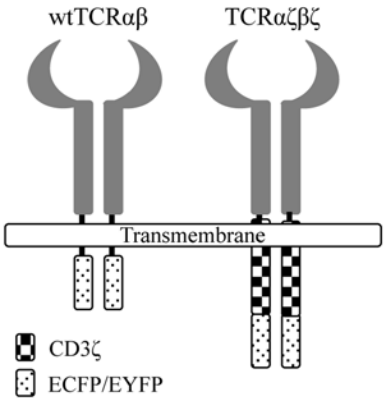

Figure 1. Schematic representation of the wild-type (wt)TCRαβ and modified TCRαζβζ variants used in the present study. wtTCRαβ was isolated from tumor infiltrating lymphocytes (TILs) of patients, the α chain was fused with enhanced cyan fluorescent protein (ECFP) and the β chain was fused with enhanced yellow fluorescent protein (EYFP). TCRαζβζ was modified by the replacement of the extracellular and transmembrane domain with CD3ζ chains, and also fused to ECFP and EYFP.

SBT in FRET efficiency measurements. The pFRET images were corrected as shown in the equation and as previously described (22): pFRET = uFRET - DSBT - ASBT, where uFRET is uncorrected FRET, ASBT is the acceptor spectral bleed-through signal, and DSBT is the donor spectral bleed-through signal. The final FRET efficiency equation was calculated as $E = 1 - I_{DA}/\{I_{DA} + pFRET \times [(\psi_{dd}/\psi_{aa}) \times (Q_d/Q_a)]\}$, where I_{DA} is the intensity of the donor in the presence of the acceptor, ψ_{dd} and ψ_{aa} are the collection efficiency in the donor and acceptor channel, and Q_d and Q_a are the quantum yield of the donor and acceptor, respectively (22,23).

Statistical analysis. Mean FRET efficiency was calculated from multiple (n=6) cell images in each group and 6 random regions of interest (ROI) in each cell image. Statistical analysis

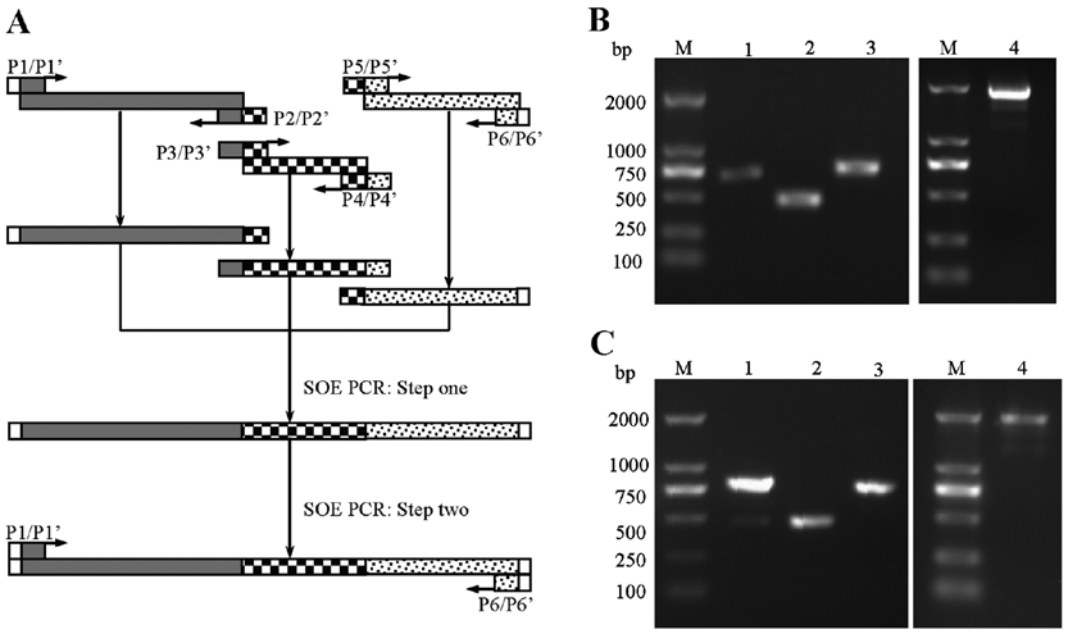

Figure 2. Generation of the fusion sequences TCRαζ-ECFP and TCRβζ-EYFP by splice overlap extension (SOE) PCR. (A) Schematic diagram of the strategy for the tripartite DNA fragment fusion. (B) PCR poducts. Left panel: lane M, molecular weight marker DL2000 (Takara); lane 1, TCRβ fragment (810 bp); lane 2, CD3ζ-b fragment (458 bp); lane 3, EYFP fragment (731 bp). Right panel: lane 4, TCRβζ-EYFP fusion (1953 bp). (C) PCR poducts. Left panel: lane 1, TCRα fragment (681 bp); lane 2, CD3ζ-a fragment (463 bp); lane 3, ECFP fragment (738 bp). Right panel: lane 4, TCRβζ-EYFP fusion (1826 bp).

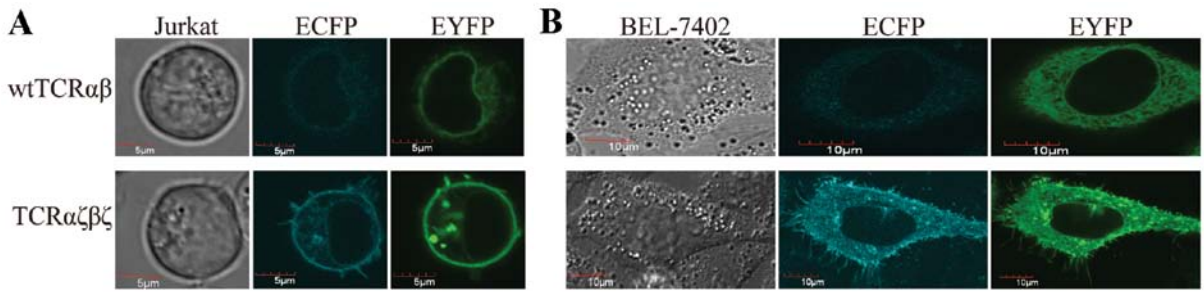

Figure 3. Expression of wild-type (wt)TCRαβ and TCRαζβζ in living cells. (A) Jurkat cells and (B) BEL-7402 cells expressing wtTCRαβ and TCRαζβζ were monitored using CLSM with FV10-ASW 1.7 software. Shown are the images in the ECFP and EYFP channels. The scale bars in Jurkat cells are 5 μm, and in BEL-7402 cells are 10 μm. All images shown are representative of at least3 independent experiments. ECFP, enhanced cyan fluorescent protein; EYFP, enhanced yellow fluorescent protein.

was performed using two-way ANOVA with a Bonferroni's multiple comparisons test using Graphpad Prism 6 software (GraphPad Software Inc., San Diego, CA, USA). Differences with P-values <0.05 were considered statistically significant. Data are expressed as the means ± SD.

Results

TCRαζβζ generation and location on the surface of cells. We designed a modified TCR in which the extracellular and transmembrane domain of TCRα or β chains were exchanged for CD3ζ chains at a structurally favorable position. To better observe the expression of the modified TCRαζβζ in living cells, we fused the C terminus of TCRαζ and TCRβζ chains to a pair of cyan and yellow fluorescent proteins, ECFP and EYFP, respectively (Fig. 1). The fusion genes, TCRαζ-ECFP and TCRβζ-EYFP, were obtained by SOE PCR (Fig. 2B and C). To compare the relative levels of surface expression with wtTCRαβ, we also fused the C terminus of the wtTCRα and wtTCRβ chains to a pair of ECFP and EYFP fluorescent proteins (Fig. 1). The fusion genes were then cloned into the pIRES2-EGFP vector.

We first examined whether the TCRαζ-ECFP and TCRβζ-EYFP fusion chains are expressed on the surface of the cells. We transfected the recombinant plasmids into Jurkat cells, as well as BEL-7402 cells, and 24 h after transfection, the fluorescence observation by CLSM revealed that the introduced fusion genes, TCRαζ-ECFP and TCRβζ-EYFP, were located at the plasma membrane of the cells and were effectively expressed in T cells and non-T cells (Fig. 3).

TCRαζβζ enhanced surface expression in T cells and non-T cells. We observed a very interesting phenomenon, namely that in the TCRαζβζ-transduced cells, but not in the TCRαβ-transduced cells, microclusters were clearly evident at the plasma membrane and the cilia of the plasma membrane

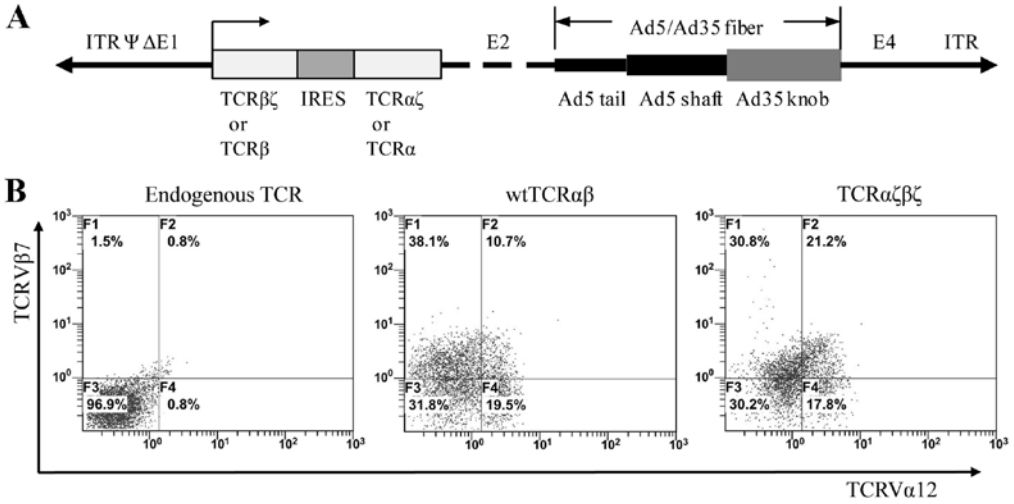

Figure 4. TCRαζβζ shows enhanced surface expression on Jurkat cells compared to wild-type (wt)TCRαβ. (A) Schematic diagram of recombinant wtTCRαβ and TCRβζαζ adenovirus. (B) Jurkat cells transduced with wtTCRαβ and TCRαζβζ stained with anti-TCR Vα12.1 mAb^{FITC} and anti-Vβ7 mAb^{PE} were analyzed by FACS.

(Fig. 3). This observation indicated that TCRαζβζ expression was stronger in the Jurkat cells and BEL-7402 cells compared to the expression of wtTCRαβ. To confirm this result, we inserted the wtTCRαβ and TCRαζβζ genes separately into the shuttle plasmid, pDC315, to produce Ad5F35 adenovirus (Fig. 4A). Ad5F35 adenovirus which contained the Ad35 fiber knob incorporated into an Ad5 capsid was able to effectively transduce human T cells. The wtTCRαβ and TCRαζβζ adenoviral vectors were introduced into the Jurkat T cells followed by FACS analysis. Double immunofluorescent staining with anti-TCRVα12 mAb^{FITC} and anti-Vβ7 mAb^{PE} showed that the Jurkat cells transduced with wtTCRαβ displayed little surface co-expression (up to 10.7%). By contrast, there was a clear increased surface coexpression (up to 21.2%) in the TCRαζβζ-transduced Jurkat cells (Fig. 4B). These data are in accordance with the imaging evidence showing the enhanced surface expression of TCRαζβζ in the cells. These results demonstrated that the FRET reporter, TCRαζ-ECFP/TCRβζ-EYFP, can be effectively used to express TCRαζβζ may thus be used for monitoring the expression and interaction of TCRαζβζ.

Highly preferred pairing between TCRαζ and βζ, but not wtTCRα and β in Jurkat cells. To investigate the interaction of TCRαζ and βζ in T cells, we used Jurkat cells (clone E6-1) expressing endogenous TCR as a recipient TCR cell model. We hypothesized that the introduced wtTCRα and β chains or TCRαζ and βζ chains composing heterodimers would result in FRET efficiency between the donor (ECFP) and acceptor (EYFP) fluorescent proteins. Once the introduced TCRαζ and βζ chains paired with endogenous TCRβ and α chains, it would fail to detect FRET between the mispaired TCR (Fig. 5C). We observed that the TCRαζβζ displayed a higher FRET signal compared to wtTCRαβ in Jurkat cells. (Fig. 5A). Six independent cell images and 6 ROI in each cell image were selected for FRET efficiency analysis in each group. The results from statistical analysis showed that the average FRET efficiency between TCRαζ-ECFP and TCRβζ-EYFP (16.7±2.5%) was significantly increased compared to wtTCRα-ECFP and wtTCRβ-EYFP (7.9±1.3%) in the Jurkat cells (P<0.0001) (Fig. 5D). These data suggested that the fusion of wtTCRα12 and β7 with CD3ζ improved pairing.

TCRαζβζ assembles independently of CD3 subunits in T cells and non-T cells. To better characterize the highly preferred pairing of TCRαζ and βζ, we selected BEL-7402 cells which are deficient in TCR and CD3 molecules as the next recipient cell model to investigate the interaction of TCRαζβζ and endogenous CD3 subunits. We hypothesized that since there was no endogenous TCR in BEL-7402 cells, the pairing of introduced wtTCRα and β or TCRαζ and βζ would not be interfered with and would result in the same FRET signal. Unexpectedly, we observed that TCRαζβζ still displayed a higher FRET signal compared to wtTCRαβ in BEL-7402 cells (Fig. 5B). The average FRET efficiency between wtTCRα and β chains (10.5±1.0%) was significantly reduced compared to the TCRαζ and βζ chains (17.1±2.1%) in BEL-7402 cells (P<0.0001) (Fig. 5D). The results indicated that the assemble of wtTCRα and β chains was impaired in the absence of CD3 subunits, in spite of no endogenous TCR in the BEL-7402 cells. Of note, we found that the average FRET efficiency between TCRαζ-ECFP and TCRβζ-EYFP in the BEL-7402 cells (17.1±2.1%) was not reduced compared to the Jurkat cells (16.7±2.5%) (P>0.05) (Fig. 5D). These results demonstrated that the expression and assembly of TCRαζβζ was not compromised even without the CD3γε, δε and ζζ signaling dimers in the BEL-7402 cells.

Discussion

In the present study, we generated several ECFP and EYFP fusions as a pair of reporters that allow the monitoring of the expression and pairing between TCRαζ and TCRβζ in living cells. First, we used a wtTCRαβ (Vα12 and Vβ7) isolated from TILs of patients fused to complete human CD3ζ molecule to generate a pair of chimeric TCRαζ and TCRβζ, then ECFP fused to TCRαζ, and EYFP fused to TCRβζ via overlap PCR,

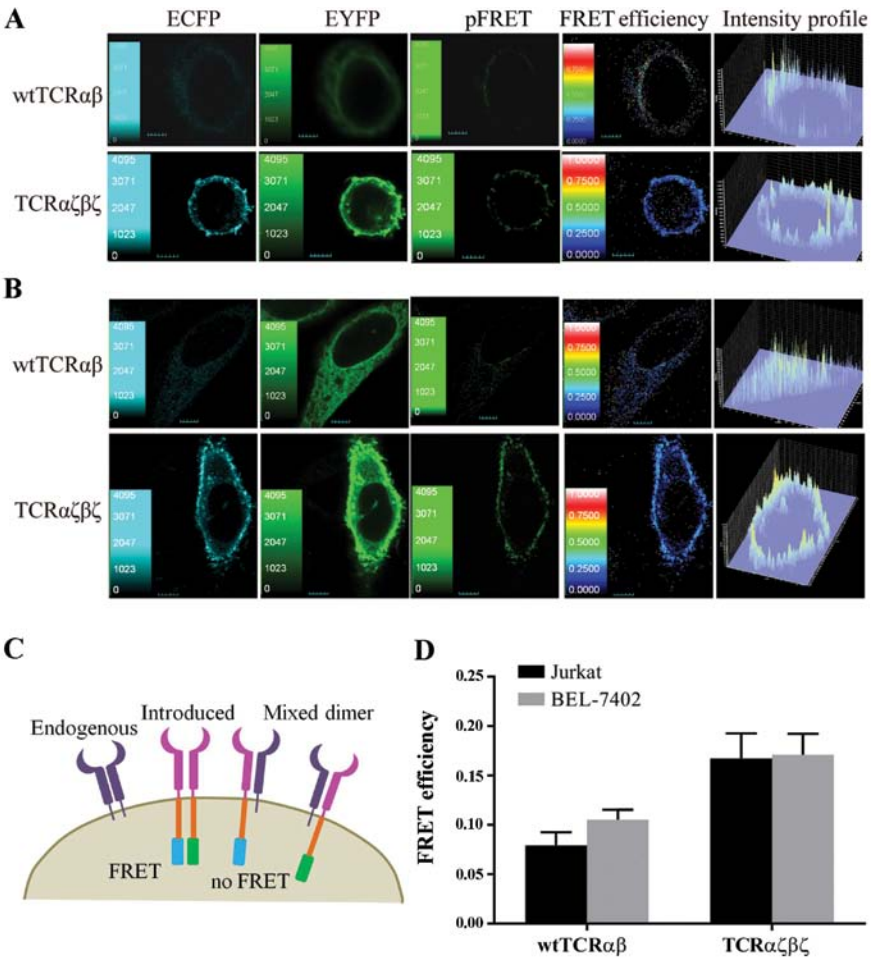

Figure 5. FRET efficiencies of wild-type (wt)TCRαβ and TCRαζβζ in living cells. Confocal images of (A) Jurkat cells and (B) BEL-7402 cells expressing wtTCRαβ or TCRαζβζ in the ECFP and EYFP channels were captured by CLSM using FV10-ASW 1.7 software, and the pFRET, FRET efficiency and intensity profile were calculated by the sensitized acceptor emission (SE) method. The continuous color scale (from black to white) represents the FRET efficiency (from 0 to 1). The scale bars in Jurkat cells are 5 μm, and in BEL-7402 cells are 10 μm. (C) Schematic diagram of pairing of TCRαζβζ chains in T cells. (D) Six independent cell images in each group and 6 random regions of interest (ROI) in each cell image were selected for the statistical analysis of FRET efficiency. Data are expressed as the means ± SD ($P<0.05$). Data represents one of 6 independent experiments with similar results. ECFP, enhanced cyan fluorescent protein; EYFP, enhanced yellow fluorescent protein.

respectively. This suggested strategy using these reporters offers several advantages over conventional immunofluorescent staining using specific antibodies: it provides accurate imaging of modified TCRαβζ expression in Jurkat T cells, and can be used in combination with FRET methods to study the interaction of TCRαζ and TCRβζ in living cells.

Using these reporters, we observed that the expression of the introduced TCRαζβζ was enhanced when compared to the non-modified wtTCRαβ in Jurkat cells, which was in line with our FACS analysis. Our results showed that the fusion gene, TCRαζβζ, coupled with ECFP/EYFP was able to be expressed normally on the surface of cells. Furthermore, we found that wtTCRαβ and TCRαζβζ were expressed not only in Jurkat cells but also in non-T cells (BEL-7402). Of note, we observed that the TCRαζβζ-transduced cells, but not the wtTCRαβ-transduced cells showed evident microclusters at the plasma membrane and cilia of the plasma membrane. These phenomena indicated that the surface expression of TCRαζβζ was markedly enhanced due to the fusion CD3ζ molecules, whereas the expression of wtTCRαβ was impaired in the absence of CD3 molecules.

The fluorescence images of the reporters were then subjected to FRET analysis which allowed the detection of the interaction of TCRαβ in the living cells. The FRET efficiencies between wtTCRα-ECFP and β-EYFP or TCRαζ-ECPF and βζ-EYFP in the Jurkat cells revealed that the introduction of TCRαζβζ improved paring compared to the wtTCRαβ majority of which mispaired with endogenous TCR. The FRET efficiency of TCRαζ and βζ in the Jurkat and BEL-7402 cells did not show any significant differences, suggesting that TCRαζβζ may be expressed/or assembled in BEL-7402 cells without endogenous CD3 subunits. The assembly of the TCR-CD3 complex is in part determined by the transmembrane charges, the positive charges at the transmembrane regions of TCRα interacting with the negative charges at the CD3δε and CD3ζζ dimers, while TCRβ interacts with CD3γε (24-26). In the TCRαζ and βζ chains, the extracellular connecting peptide motif, transmembrane and intracellular domains of TCRα and β are replaced by CD3ζ. Thereby, CD3γε or CD3δε cannot be associated with the modified TCRαζβζ, which explains why TCRαζβζ can expressed independently of CD3 components.

In conclusion, using the strategy of fluorescent proteins fused to the TCRαζ and βζ chains we monitored and measured the expression and interaction of TCRαζ and TCRβζ in living cells accurately. The ECFP and EYFP fusion reporters revealed that the TCRαβ chains fused to CD3ζ enhanced the expression and prevented mispairing, paving the way to potential immunological studies dealing with TCR mispairing.

Acknowledgements

The present study was supported by grants from the National Natural Science Foundation of China (nos. 31100664, 31300737 and 81303292), the National Major Scientific and Technological Special Project for 'Significant New Drugs Development' (no. 2009ZX09103-708), the Natural Science Foundation of Guangdong Province (no. 10151022401000024), and a grant from the Faculty Development and Research Funds of GDPU and The Science and Technology Research Project of Dongguan City (no. 2011105102027).

References

1. Heemskerk MH, Hoogeboom M, Hagedoorn R, *et al*: Reprogramming of virus-specific T cells into leukemia-reactive T cells using T cell receptor gene transfer. J Exp Med 199: 885-894, 2004.
2. Hughes MS, Yu YY, Dudley ME, *et al*: Transfer of a TCR gene derived from a patient with a marked antitumor response conveys highly active T-cell effector functions. Hum Gene Ther 16: 457-472, 2005.
3. Abad JD, Wrzensinski C, Overwijk W, *et al*: T-cell receptor gene therapy of established tumors in a murine melanoma model. J Immunother 31: 1-6, 2008.
4. Coccoris M, Swart E, de Witte MA, *et al*: Long-term functionality of TCR-transduced T cells in vivo. J Immunol 180: 6536-6543, 2008.
5. de Witte MA, Bendle GM, van den Boom MD, *et al*: TCR gene therapy of spontaneous prostate carcinoma requires in vivo T cell activation. J Immunol 181: 2563-2571, 2008.
6. Dossett ML, Teague RM, Schmitt TM, *et al*: Adoptive immunotherapy of disseminated leukemia with TCR-transduced, $CD8^+$ T cells expressing a known endogenous TCR. Mol Ther 17: 742-749, 2009.
7. Morgan RA, Dudley ME, Wunderlich JR, *et al*: Cancer regression in patients after transfer of genetically engineered lymphocytes. Science 314: 126-129, 2006.
8. Johnson LA, Morgan RA, Dudley ME, *et al*: Gene therapy with human and mouse T-cell receptors mediates cancer regression and targets normal tissues expressing cognate antigen. Blood 114: 535-546, 2009.
9. Bendle GM, Linnemann C, Hooijkaas AI, *et al*: Lethal graft-versus-host disease in mouse models of T cell receptor gene therapy. Nat Med 16: 565-570, 2010.
10. van Loenen MM, de Boer R, Amir AL, *et al*: Mixed T cell receptor dimers harbor potentially harmful neoreactivity. Proc Natl Acad Sci USA 107: 10972-10977, 2010.
11. Cohen CJ, Zhao Y, Zheng Z, *et al*: Enhanced antitumor activity of murine-human hybrid T-cell receptor (TCR) in human lymphocytes is associated with improved pairing and TCR/CD3 stability. Cancer Res 66: 8878-8886, 2006.
12. Sommermeyer D and Uckert W: Minimal amino acid exchange in human TCR constant regions fosters improved function of TCR gene-modified T cells. J Immunol 184: 6223-6231, 2010.
13. Kuball J, Dossett ML, Wolfl M, *et al*: Facilitating matched pairing and expression of TCR chains introduced into human T cells. Blood 109: 2331-2338, 2007.
14. Cohen CJ, Li YF, El-Gamil M, *et al*: Enhanced antitumor activity of T cells engineered to express T-cell receptors with a second disulfide bond. Cancer Res 67: 3898-3903, 2007.
15. Voss RH, Willemsen RA, Kuball J, *et al*: Molecular design of the Cαβ interface favors specific pairing of introduced TCRαβ in human T cells. J Immunol 180: 391-401, 2008.
16. Willemsen R, Weijtens M, Ronteltap C, *et al*: Grafting primary human T lymphocytes with cancer-specific chimeric single chain and two chain TCR. Gene Ther 7: 1369-1377, 2000.
17. Zhang T, He X, Tsang TC, *et al*: Transgenic TCR expression: comparison of single chain with full-length receptor constructs for T-cell function. Cancer Gene Ther 11: 487-496, 2004.
18. Schaft N, Lankiewicz B, Drexhage J, *et al*: T cell re-targeting to EBV antigens following TCR gene transfer: CD28-containing receptors mediate enhanced antigen-specific IFNγ production. Int Immunol 18: 591-601, 2006.
19. Wu F, Zhang W, Shao H, *et al*: Human effector T cells derived from central memory cells rather than $CD8^+$ T cells modified by tumor-specific TCR gene transfer possess superior traits for adoptive immunotherapy. Cancer Lett 339: 195-207, 2013.
20. Shao H, Zhang W, Hu Q, *et al*: TCR mispairing in genetically modified T cells was detected by fluorescence resonance energy transfer. Mol Biol Rep 37: 3951-3956, 2010.
21. Schroers R, Hildebrandt Y, Hasenkamp J, *et al*: Gene transfer into human T lymphocytes and natural killer cells by Ad5/F35 chimeric adenoviral vectors. Exp Hematol 32: 536-546, 2004.
22. Elangovan M, Wallrabe H, Chen Y, *et al*: Characterization of one-and two-photon excitation fluorescence resonance energy transfer microscopy. Methods 29: 58-73, 2003.
23. Wallrabe H and Periasamy A: Imaging protein molecules using FRET and FLIM microscopy. Curr Opin Biotech 16: 19-27, 2005.
24. Call ME, Wucherpfennig KW and Chou JJ: The structural basis for intramembrane assembly of an activating immunoreceptor complex. Nat Immunol 11: 1023-1029, 2010.
25. Kuhns MS, Girvin AT, Klein LO, *et al*: Evidence for a functional sidedness to the αβTCR. Proc Natl Acad Sci USA 107: 5094-5099, 2010.
26. Call ME, Schnell JR, Xu C, *et al*: The structure of the ζζ transmembrane dimer reveals features essential for its assembly with the T cell receptor. Cell 127: 355-368, 2006.